Polymorphic Behavior of Syndiotactic Polystyrene Crystallized in Cylindrical Nanopores

Hui Wu,[†] Wei Wang,[†] Yan Huang,[†] Cheng Wang,[‡] and Zhaohui Su*,[†]

State Key Laboratory of Polymer Physics and Chemistry and State Key Laboratory of Rare Earth Resources Utilization, Changchun Institute of Applied Chemistry, Chinese Academy of Sciences, Changchun, Jilin 130022, P. R. China

Received July 6, 2008
Revised Manuscript Received August 18, 2008

Introduction

Structure and morphology of polymers under nanoscale confinement have attracted considerable interest recently. For semicrystalline polymer materials, the degree of crystallinity and the orientation of the crystalline domains are important factors in controlling their physical properties, and many efforts have been devoted to the understanding of the crystallization and orientation behavior of polymers in one-,[1−4] two-,[5−14] or three-dimensional[15−18] confinements. For example, in 1D confinement, an extensive reduction in crystallinity and a reduction in the rate of crystallization were reported for ultrathin films;[1] the backbone of poly(di-*n*-hexylsilane) lied extended with the polymer axis parallel to the plane of the film, while the side chains were extended with their carbon plane mostly perpendicular to the substrate.[2] In 2D confinements, i.e. in nanocylindrical geometry, polymers inside organic[5−8] or inorganic[9−13] templates exhibit preferred orientation. Studies on the crystallization of poly(ethylene oxide) (PEO) confined in nanocylinders indicate that the orientation of the PEO crystals is dependent on the crystallization temperature.[6,7] The crystals in the nanorods crystallized at low supercooling exhibit a perpendicular orientation,[8−12] and the crystallinity is reduced in contrast to the bulk.[11,12] In nanotrenches PVDF crystals were found to orient with the chain axis parallel to the walls.[14] For polymer under 3D confinements, nanoscale polyethylene spheres[15] and PEO droplets[16] were investigated, and in both cases the crystallization was initiated by homogeneous nucleation, which is much different from that for typical polymers in the bulk where heterogeneous nucleation dominates. Homogeneous nucleation within each nanosphere led to isothermal crystallization which followed first-order kinetics.[15] In addition, it has been reported that for the crystallization of semiflexible homopolymers confined in isolated nanodomains nucleation occurs predominantly at the domain interface, and the domain interface accelerates the process.[17] In addition to experimental results, dynamic Monte Carlo simulation has been applied to study polymer crystallization under cylindrical confinement.[19−21]

It is well-known that anodic aluminum oxide (AAO) membranes consisting of ordered straight separated cylindrical pores are ideal templates for the fabrication of polymer nanorods and for morphological study of polymers under cylindrical confinement.[9−13] The thermal stability and mechanical rigidity of the alumina wall provide a strictly constrained environment and avoid the breakdown of the cylindrical confinement. The characteristic feature size and shape of the nanomaterial are easily controlled by the distribution of the template pores, and thus the mechanical, optical, and electrical properties of the polymer are largely determined by the internal morphology.

Syndiotactic polystyrene (sPS) is a semicrystalline polymer that has received considerable academic and industrial attention owing to its desirable physical properties such as high stiffness both above and below the glass transition temperature, good thermal and chemical stability, and low dielectric constant.[22,23] It exhibits rapid crystallization rate, high crystallinity, and high melting temperature due to the high stereoregularity of the polymer chain.[23] Of particular interest is that sPS exhibits complicated polymorphic behavior involving four identified crystalline forms: α, β, γ, and δ. It has been shown that the γ- and δ-forms possess s(2/1)2 helical chain conformation of regular repetition of TTGG, while the α- and β-forms both contain planar zigzag chains (TTTT conformation).[24] The polymorphism of this polymer is strongly dependent on the thermal and solvent treatment.[25] Typically, α-form is favored under the conditions of fast cooling from the melt to room temperature,[24] or melt crystallization at low temperatures (<230 °C),[26] or cold crystallization from quenched glass.[24] On the other hand, the β-form can be obtained by either slow cooling from the melt,[27] or growth from solution,[27] or transformation from other crystal forms (δ, γ, or α) with the plasticization of the solvents.[25,28−30]

In our previous work, we studied the crystallization of sPS in the nanopores of 200 and 80 nm using FTIR and TEM, and it was found that at low supercooling only β-crystals formed in the nanorods with the *c*-axis aligning perpendicular to the axial direction of the nanorod, and the degree of crystallinity was significantly lower than that in the bulk.[11] In order to explore the morphology and phase behavior of the polymer under stronger confinement conditions, in the present work we prepared sPS nanorods with diameter of 32 nm using AAO templates and investigated the crystallization and polymorphic behavior of the polymer in the cylindrical nanopores.

Experimental Section

SPS pellets (Dow Questra F-2250, $M_w = 2.6 \times 10^5$, $M_w/M_n = 2.0$) were used as received. A transparent amorphous sPS film with thickness of ~180 μm was obtained by compression molding several sPS pellets at 300 °C and quickly quenching the film in ice water. The AAO templates with 32 nm pore diameter and 90 μm pore depth were prepared via a two-step anodization process using oxalic acid as the electrolyte. Details of the anodization process can be found elsewhere.[31] Prior to use, the templates were ultrasonicated in solvents of different polarity, such as deionized water, ethanol, chloroform, and acetone, for 2 min each. In order to study the polymorphic and crystallization behavior of the polymer confined within the 32 nm nanopores, nanorods with different thermal histories were prepared. An alumina membrane was placed on top of the sPS film supported by a glass slide, and the assembly was heated at 300 °C for 1.5 h under a nitrogen atmosphere so that the sPS melt was drawn into the membrane pores by capillary force. The assembly was cooled down from molten state to 255 °C quickly and crystallized at this temperature for 2 h and then cooled to room temperature slowly in a homemade temperature controller (cooling rate less than 1 °C/min) (sample A). Sample B was crystallized from the molten state at 255 °C for 2 h and then quenched in ice water. Sample C was obtained by annealing sample B at 255 °C for 2 h again and then cooled to room temperature in the temperature controller slowly. Sample D was crystallized from the

* To whom all correspondence should be addressed: Tel (86)431-85262854; Fax (86)431-85262126; e-mail zhsu@ciac.jl.cn.
† State key Laboratory of Polymer Physics and Chemistry.
‡ State Key Laboratory of Rare Earth Resources Utilization.

10.1021/ma801498b CCC: $40.75
Published on Web 09/27/2008

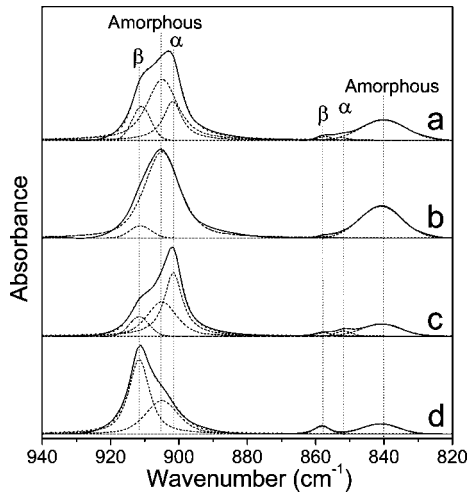

Figure 1. Infrared spectra of the nanorods in sample A (a), sample B (b), sample C (c), and a bulk film (d). The dash lines are the deconvoluted peaks, and the dotted lines are the fitted curves.

Table 1. Comparison of the Percent Crystallinity for the Samples with Various Thermal Histories

	nanorods		bulk
sample	C_α	C_β	C_β
sample A: 255 °C for 2 h and slow cooling	26.0	13.3	60.2
sample B: 255 °C for 2 h and quenched	0	10.4	55.3
sample C: sample B heated at 255 °C for 2 h and slow cooling	43.3	12.1	62.5
sample D: 255 °C for 6 h and quenched	0	10.3	54.6

melt at 255 °C for 6 h and then quenched in ice water. For microscopy and FTIR measurements, the template/polymer assembly was immersed in a sodium hydroxide aqueous solution to remove the AAO template, leaving an array of sPS nanorods protruding from the sPS film. Thin slices of the cross section of a sPS film with protruding nanorods were cut under an optical microscope using a razor blade. For XRD and DSC studies, the bulk film in connection with the nanorods was mechanically removed by a sharp blade carefully, and this side of the template was further blasted with oxygen plasma for 20 min at 100 W to ensure that the residual bulk sPS was removed.

Details of experimental procedures for FTIR and SEM can be found in our previous report.[11] X-ray diffraction (XRD) patterns of the nanorods insid the AAO template were collected on a Bruker D8 Discover X-ray reflectometer equipped with a Cu Kα radiation source ($\lambda = 0.154$ nm). The diffraction data were collected from $2\theta = 4-28°$ in a locked coupled scan type with a scan speed of 0.5 deg/min and a 0.05° increment. A TA Instruments Q-100 calorimeter was employed to study the nucleation behavior of the nanorods inside the AAO template. The temperature was calibrated using an indium standard. The cooling runs from 310 to 30 °C were scanned at 10 °C/min under nitrogen purge.

Results and Discussion

The sPS nanorods of 32 nm diameter were first examined by FTIR. The 940−820 cm^{-1} region where the bands characteristic of different morphology are observed[32] of the FTIR spectra for the nanorods and the bulk is shown in Figure 1. For bulk sPS, except the amorphous bands at 905 and 841 cm^{-1}, the only other bands present are at 911 and 858 cm^{-1}, characteristic of the β-form crystallinity, which is verified by examining the second derivative of the spectra (not shown), indicating that the crystalline phase in the bulk was the β-form, which is consistent with the literature.[32] On the other hand, in the spectrum of the nanorods of sample A, in addition to the four bands observed for the bulk characteristic of the amorphous and the β-phases as discussed above, two bands characteristic of the α crystallinity at 901 and 851 cm^{-1} also emerge, indicating the coexistence of α- and β-crystalline phases in the nanorods. The crystallinity was then determined,[11,32] and it was found that the crystallinity in the bulk was 60.2% in the β-form, and in the 32 nm nanorods the α-form and β-form were 26.0% and 13.3%, respectively (see Table 1). Thus, compared with that in the bulk and in the nanorods of larger diameters, the sPS exhibited much lower crystallinity in the nanorods of 32 nm diameter.

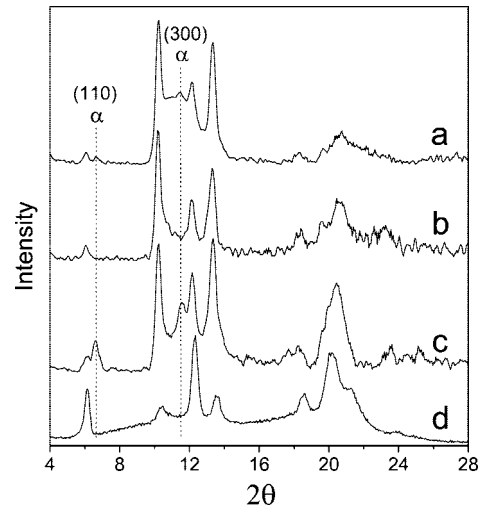

Figure 2. X-ray diffraction patterns of the nanorods in sample A (a), sample B (b), sample C (c), and a bulk film (d).

It is known that in the bulk state sPS crystallizes from the melt at high temperatures (low supercooling) into only β-crystals,[27,33] while α crystallinity is resulted from fast cooling to room temperature from the melt,[24] cold crystallization from quenched glass,[24] or melt crystallization at low temperatures.[26] Since the nanorods and the bulk film were connected and treated together, they experienced the same thermal history and had the same crystallization conditions except that the polymer chains in the nanorods were under the confinement of the nanotemplate. In order to understand the difference observed in the crystallization and polymorphic behavior for the sPS in the nanotemplate and in the bulk, two more samples (samples B and C) were investigated. In the spectrum for the rapidly quenched nanorods (sample B) the β characteristic bands at 858 and 911 cm^{-1}, although small are clearly identified, while the 901 and 851 cm^{-1} bands characteristic of the α-phase are absent. On the other hand, the IR spectrum for the nanorods in sample C indicates the presence of both α- and β-crystalline phases.

Figure 2 shows the XRD patterns of the 32 nm nanorods with different thermal histories and the bulk as a reference. For the nanorods in sample B and the bulk sPS, diffraction peaks are observed at $2\theta = 6.1°$ (020), 10.3° (110), 12.3° (040), 13.6° (130), and 18.6° (060), showing that the crystalline phase is in the β-form.[24] In the XRD patterns of the nanorods in sample A and sample C, in addition to the peaks attributed to the β-form, two new peaks at $2\theta = 6.7°$ (110) and $2\theta = 11.7°$ (300), characteristic of the α-form sPS,[24] appear. This result is consistent with the FTIR data, showing that in the nanorods of sample A and sample C both α- and β-crystalline phases are present.

The degrees of crystallinity for both nanorods and the bulk in these various samples were then extracted from the IR data,[11,32] and the numbers are listed in Table 1. First we compare the crystallinity between sample B and sample D, which were

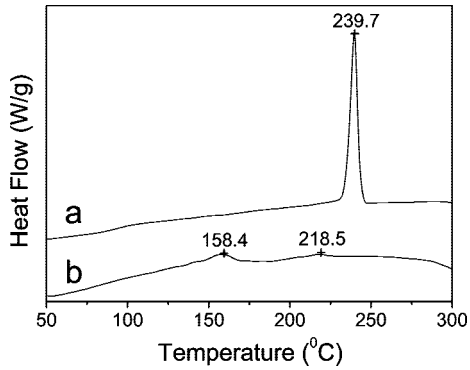

Figure 3. DSC cooling runs of (a) a bulk sPS film and (b) separated sPS nanorods within the AAO template of 32 nm diameter.

crystallized at 255 °C for 2 and 6 h, respectively. Only the β-phase was present in both nanorods and the bulk for these two samples, and the degree of crystallinity was the same for the two nanorods at ~10% and the same for the bulk at ~55%. This result suggests that the crystallization process at 255 °C was complete within 2 h either in the 32 nm nanorods or in the bulk, which is due to the rapid crystallization rate of sPS at this temperature.[34] That while there were still large amount of crystallizable chain segments in the amorphous phase, the crystallization process finished at a low degree of crystallinity of ~10% compared to ~55% in the bulk and extended annealing did not lead to more crystalline content suggests that the crystallization in the nanorods was dominated by heterogeneous nucleation. This then indicates that the difference in the β-crystallinity we observed in the 32 nm nanorods and the bulk was not due to incomplete crystallization process in the template. According to our previous study,[11] for sPS crystallizes at low supercoolings, this great reduction in β-crystallinity in nanorods is due to the constrain of the nanotemplate to the growth of the crystallites. More dramatic reduction (~45%) was observed here for the 32 nm nanorods compared with that for nanorods of greater diameters,[11] apparently because of the stronger constrain imposed by smaller pore diameter. Then by comparing sample A with sample B, it is immediately clear that the α-crystals in the nanorods were produced in the slow cooling down from 255 °C to room temperature. It is interesting to find that the amount of β-phase in both slowly cooled samples (A and C) was slightly higher than that in the quickly quenched ones (B and D) in both the bulk and the nanorods. The difference was ~2−3% for the nanorods and ~5−7% for the bulk. This is because of further β-crystallization at >230 °C in the cooling process.[33] It is also noticed that the α-content in the nanorods in sample C was much higher than that in sample A, and this is attributed to the cold crystallization of sPS in the extra reheating step sample C went through.

The DSC cooling runs for the sPS nanorods located inside the 32 nm template and the bulk as a reference are shown in Figure 3. A sharp crystallization peak at 239.7 °C is found for the sPS in the bulk, but the nanorods exhibit two broad and weak peaks at 218.5 and 158.4 °C. While it is known that for semicrystalline polymers the crystallization at low supercooling in the bulk typically is initiated by heterogeneous nucleation, it has been reported that both heterogeneous and homogeneous nucleation contributed to the crystallization of polyethylene in AAO templates with pore diameters of 33−48 nm,[13] where two crystallization exotherms were observed by DSC similar to what we found for the sPS nanorods. Therefore, for the nanorods, the first weaker peak at 218.5 °C is attributed to the crystallization via heterogeneous nucleation, while the peak at 158.4 °C, which is about 80 °C lower than the crystallization peak for the bulk (i.e., much deeper supercooling in the nanorods than in the bulk), suggests that the crystallization of the confined and isolated polymer in the smaller pores at this stage is more likely initiated by homogeneous nucleation.

With the above results, we are now in a position to summarize the crystallization and polymorphic behavior of sPS in 32 nm nanorods in contrast to that in the bulk. In the bulk state, it is known that β-crystalline state is favored over the α-state at high crystallization temperatures, and the polymorph of sPS is the competition between thermodynamics and kinetics during the crystallization process; the crystalline α-form is kinetically favorable while the crystalline β-form is thermodynamically favorable.[24] It is well recognized that at low cooling rates the crystalline phase of β-form has almost reached the maximum crystallinity of the sample by cooling to 230 °C, and there is no more crystallizable sPS portion remained for the α-form formation during its further cooling to room temperature.[33] Therefore, in the bulk of the sPS crystallization is dominated by heterogeneous nucleation and occurs at higher temperatures, leading to β-form exclusively with high degree of crystallinity. On the other hand, in the nanorods β-phase is formed via heterogeneous nucleation, but the growth of the stable β-form crystallites in the nanopores is restricted compared to that in the bulk due to the cylindrical confinement of the pores with small diameter, resulting in much lower β-crystallinity in the nanorods at high temperatures; while there are still large amount of potentially crystallizable chain segments in the amorphous state, there is no more nuclei at this temperature. Then upon slow cooling to room temperature, the crystallizable chain segments nucleate again and grow into the less stable α-crystals at lower temperatures, and this process is dominated by homogeneous nucleation.

Conclusions

In this work we have studied the polymorphic and crystallization behavior of syndiotactic polystyrene (sPS) in the cylindrical nanopores of 32 nm diameter. For sPS annealed at low supercoolings in the bulk, without any geometric constrain, via heterogeneous nucleation the polymer can crystallize to an extent as determined by the temperature, resulting in β-crystallinity exclusively of high content. In the nanorods, via the same heterogeneous nucleation the polymer crystallizes into β-form at low supercoolings, but because of the confinement of the nanopores the growth of the crystallites is restricted, resulting in a much lower β-content and leaving large portions of crystallizable chain segments in the amorphous phase which can then further crystallize upon slow cooling, mainly into the α-form via homogeneous nucleation, and a mixture of α- and β-crystalline phases is produced. These results may help researchers better understand the crystallization behavior of polymers under confinement.

Acknowledgment. We thank National Natural Science Foundation of China (20774097, 20423003) for financial support and Dr. Dorie Yontz of Dow Chemical Co. for supplying the sPS used in this study. Z.S. thanks the NSFC Fund for Creative Research Groups (50621302) for support.

Supporting Information Available: FE-SEM images of the AAO templates with a pore diameter of 32 nm and the nanorods prepared. This material is available free of charge via the Internet at http://pubs.acs.org.

References and Notes

(1) Schönherr, H.; Frank, C. W. *Macromolecules* **2003**, *36*, 1188.
(2) Despotopoulou, M. M.; Miller, R. D.; Rabolt, J. F.; Frank, C. W. *J. Polym. Sci., Part B: Polym. Phys.* **1996**, *34*, 2335.
(3) Zhu, L.; Cheng, S. Z. D.; Calhoun, B. H.; Ge, Q.; Quirk, R. P.; Thomas, E. L.; Hsiao, B. S.; Yeh, F. J.; Lotz, B. *J. Am. Chem. Soc.* **2000**, *122*, 5957.
(4) Sun, Y. S.; Chung, T. M.; Li, Y. J.; Ho, R. M.; Ko, B. T.; Jeng, U. S.; Lotz, B. *Macromolecules* **2006**, *39*, 5782.
(5) Quiram, D. J.; Register, R. A.; Marchand, G. R.; Adamson, D. H. *Macromolecules* **1998**, *31*, 4891.
(6) Huang, P.; Zhu, L.; Cheng, S. Z. D.; Ge, Q.; Quirk, R. P.; Thomas, E. L.; Lotz, B.; Hsiao, B. S.; Liu, L. Z.; Yeh, F. J. *Macromolecules* **2001**, *34*, 6649.
(7) Huang, P.; Guo, Y.; Quirk, R. P.; Ruan, J. J.; Lotz, B.; Thomas, E. L.; Hsiao, B. S.; Avila-Orta, C. A.; Sics, I.; Cheng, S. Z. D. *Polymer* **2006**, *47*, 5457.
(8) Liu, Y.; Cui, L.; Guan, F. X.; Gao, Y.; Hedin, N. E.; Zhu, L.; Fong, H. *Macromolecules* **2007**, *40*, 6283.
(9) Steinhart, M.; Senz, S.; Wehrspohn, R. B.; Gösele, U.; Wendorff, J. H. *Macromolecules* **2003**, *36*, 3646.
(10) Steinhart, M.; Goring, P.; Dernaika, H.; Prabhukaran, M.; Gösele, U.; Hempel, E.; Thurn-Albrecht, T. *Phys. Rev. Lett.* **2006**, *97*, 027801.
(11) Wu, H.; Wang, W.; Yang, H.; Su, Z. *Macromolecules* **2007**, *40*, 4244.
(12) Shin, K.; Woo, E.; Jeong, Y. G.; Kim, C.; Huh, J.; Kim, K. W. *Macromolecules* **2007**, *40*, 6617.
(13) Woo, E.; Huh, J.; Jeong, Y. G.; Shin, K. *Phys. Rev. Lett.* **2007**, *98*, 136103.
(14) Hu, Z. J.; Baralia, G.; Bayot, V.; Gohy, J. F.; Jonas, A. M. *Nano Lett.* **2005**, *5*, 1738.
(15) Loo, Y. L.; Register, R. A.; Ryan, A. J. *Phys. Rev. Lett.* **2000**, *84*, 4120.
(16) Massa, M. V.; Dalnoki-Veress, K. *Phys. Rev. Lett.* **2004**, *92*, 255509.
(17) Nojima, S.; Ohguma, Y.; Namiki, S.; Ishizone, T.; Yamaguchi, K. *Macromolecules* **2008**, *41*, 1915.
(18) Jiang, S. C.; Ji, X. L.; An, L. J.; Jiang, B. Z. *Polymer* **2001**, *42*, 3901.
(19) Wang, M. X.; Hu, W. B.; Ma, Y.; Ma, Y. Q. *J. Chem. Phys.* **2006**, *124*, 244901.
(20) Miura, T.; Mikami, M. *Phys. Rev. E* **2007**, *75*, 031804.
(21) Ma, Y.; Hu, W. B.; Hobbs, J.; Reiter, G. *Soft Matter* **2008**, *4*, 540.
(22) Ishihara, N.; Seimiya, T.; Kuramoto, M.; Uoi, M. *Macromolecules* **1986**, *19*, 2464.
(23) Su, Z.; Hsu, S. L.; Li, X. *Macromolecules* **1994**, *27*, 287.
(24) Guerra, G.; Vitagliano, V. M.; De Rosa, C.; Petraccone, V.; Corradini, P. *Macromolecules* **1990**, *23*, 1539.
(25) Handa, Y. P.; Zhang, Z. Y.; Wong, B. *Macromolecules* **1997**, *30*, 8499.
(26) Sun, Y. S.; Woo, E. M. *Macromolecules* **1999**, *32*, 7836.
(27) De Rosa, C.; Rapacciuolo, M.; Guerra, G.; Petraccone, V.; Corradini, P. *Polymer* **1992**, *33*, 1423.
(28) Ma, W. M.; Yu, J.; He, J. S. *Macromolecules* **2005**, *38*, 4755.
(29) Gowd, E. B.; Shibayama, N.; Tashiro, K. *Macromolecules* **2007**, *40*, 6291.
(30) Gao, X.; Liu, R.; Huang, Y.; Starykov, O.; Oppermann, W. *Macromolecules* **2008**, *41*, 2554.
(31) Masuda, H.; Fukuda, K. *Science* **1995**, *268*, 1466.
(32) Wu, H. D.; Wu, I. D.; Chang, F. C. *Macromolecules* **2000**, *33*, 8915.
(33) Bu, W. S.; Li, Y. Y.; He, J. S.; Zeng, J. J. *Macromolecules* **1999**, *32*, 7224.
(34) Wu, T. M.; Hsu, S. F.; Chien, C. F.; Wu, J. Y. *Polym. Eng. Sci.* **2004**, *44*, 2288.

MA801498B